chemosensors

MDPI

Article

In Vitro and *In Silico* Evaluation of Indole-Bearing Squaraine Dyes as Potential Human Serum Albumin Fluorescent Probes

Margarida A. Sousa [1,†], Eurico Lima [1,2,†], Octávio Ferreira [2], Renato E. Boto [2], Paulo Almeida [2] and Lucinda V. Reis [1,*]

[1] Chemistry Centre of Vila Real (CQVR), University of Trás-os-Montes and Alto Douro, Quinta de Prados, 5001-001 Vila Real, Portugal
[2] Health Sciences Research Centre (CICS-UBI), University of Beira Interior, Av. Infante D. Henrique, 6201-001 Covilhã, Portugal
* Correspondence: lucinda.reis@utad.pt
† These authors contributed equally to this work.

Abstract: The quantitative determination of proteins is an important parameter in biochemistry, biotechnology and immunodiagnostics, and the importance of serum albumin in clinical diagnosis should be highlighted, given that alterations in its concentration are generally associated with certain diseases. As possible probes for this purpose, squaraine dyes have been arousing the interest of many researchers due to their unique properties, such as absorption in the visible spectra, moderate relative fluorescence quantum yields and increased fluorescence intensity after non-covalent binding to specific ligands. In this work, five squaraine dyes, four of which have never been reported in the literature, were characterized and evaluated *in vitro* and *in silico* concerning their potential application as fluorescent probes for human serum albumin detection. After interaction with the protein, the fluorescence intensity increased from 12 to 41 times, depending on the dye under study. High sensitivity (1.0×10^5–5.4×10^5 nM), low detection limits (168–352 nM) and moderate quantitation limits (560–1172 nM) were obtained, proving the efficiency of the method. In addition, moderate-to-excellent selectivity was observed compared to γ-globulin proteins. Molecular docking suggests that the dyes interact more effectively with the Sudlow site I, and binding energies have been markedly higher than those of warfarin, a molecule known to bind to this site specifically.

Keywords: human serum albumin; squaraine dyes; computational analysis; *in vitro* studies; fluorescent probes

Citation: Sousa, M.A.; Lima, E.; Ferreira, O.; Boto, R.E.; Almeida, P.; Reis, L.V. *In Vitro* and *In Silico* Evaluation of Indole-Bearing Squaraine Dyes as Potential Human Serum Albumin Fluorescent Probes. *Chemosensors* **2022**, *10*, 314. https://doi.org/10.3390/chemosensors10080314

Academic Editors: Guo-Hui Pan, Hongshang Peng and Biao Dong

Received: 22 June 2022
Accepted: 3 August 2022
Published: 6 August 2022

1. Introduction

Human serum albumin (HSA) is the most abundant protein in the human circulatory system, is synthesized in the liver, and represents about 52% of the blood's composition [1]. Due to their high bioavailability, low cost, stability, and ability to transport different ligands to specific sites, these proteins have been the most widely studied over the last few years [2,3]. Within its main functions, the transport of various macromolecules such as hormones, lipids, metal ions, amino acids, and some drugs in the body [4] is the most relevant. Thus, albumin plays an essential role in maintaining metabolic processes, such as determining oncotic plasma pressure, decreasing some toxins' activity, and controlling the plasma's antioxidant properties [5,6].

Quantifying proteins in biological fluids has shown great interest in several areas, such as biochemistry, biotechnology, and immunodiagnostics [7]. Since serum albumins are the main soluble protein constituents of the circulatory system, their quantification in biomedical diagnostics is a fundamental parameter in assessing a patient's health status [8]. For example, changes in blood albumin levels can be used as a biomarker at an early stage of various disorders, such as of a cardiovascular origin, liver disease, nephrotic

syndrome, diabetes, and severe dehydration [1,9]. Currently, there are several protein-detection methods, namely, colorimetric techniques, such as the Lowry and Bradford methods, immunoassays, cyclic voltammetry, and chemiluminescence. However, these more traditional methods present certain limitations, such as a long reaction time and the need for specific equipment and specialized personnel, increasing the cost of the processes and even creating complicated sample preparation protocols [10,11].

The development of new methods that can overcome these disadvantages and offer a faster, low-cost, and non-invasive evaluation has been an area of great interest. One of the alternatives is fluorescence spectroscopy, which has several advantages, such as high sensitivity, selectivity, simplicity, and compatibility with live cells and physiological assays, and allows for the real-time detection of proteins [12–14]. Several detection methods based on fluorescence have been developed in clinical and biological research [11], and several fluorescent dyes are commercially available, such as ethidium bromide, eosin B and eosin Y, albumin blue, and Coomassie Brilliant Blue [1].

Several fluorescent probes developed in recent years for the detection of serum albumins *in vitro* or *in vivo* have a low excitation wavelength (<500 nm), an emission wavelength < 600 nm, and a detection limit >30 mg/L, also showing photodegradation and interference caused by the autofluorescence of biomolecules, which limits their biological application in complex body fluids. Thus, it has been increasingly important to develop fluorescent probes that absorb in the red and near-infrared (NIR) region (>650 nm), which have high selectivity, sensitivity, stability, and a low detection limit for the recognition of serum albumins in biological samples [15,16]. In 2020, as an example, Aristova et al. [17] reported a study in which benzothiazole-derived pentamethine cyanines were evaluated for their potential application as fluorescent probes for serum albumins. These dyes exhibited maximum absorption near 600 nm and improved interaction with serum albumins compared to other globular proteins.

In addition to other biomedical applications, squaraine dyes have been used in the research on sensors to detect different types of analytes. Due to its strong absorption and emissions, it was possible to develop selective fluorescent probes for metal ions, explosives (such as picric acid [18]), and other important molecules. In the literature, there are a variety of dyes capable of selectively detecting some ions such as mercury [19,20], iron [21,22], copper [23,24], zinc [25,26], lead [27], sodium [28], silver [29], magnesium [30], and chloride [31,32]. The detection of metal ions has proved to be of great importance since they are not biodegradable and tend to accumulate in living organisms, and some heavy metals are known to be toxic and carcinogenic [33]. Some dyes are susceptible to the hydroxide ion and function as pH sensors [34,35].

In the recent literature, there are studies by Butnarasu et al. [36,37] where the authors evaluated the interaction of squaraine dyes with some proteins such as gastric mucins, transferrin, fibrinogen, trypsin, pepsin, and a gastric protease, to understand better the behavior of these compounds in the presence of different proteins and obtain helpful information in the development of new, more effective, and selective fluorescent dyes. In addition, intracellular biothiols, such as glutathione [38,39], cysteine, and homocysteine [39,40], are other components of biological systems which can be detected through the use of squaraines. Furthermore, since alterations in the levels of these components are strongly associated with diseases, such as Alzheimer's, liver damage [41], cardiovascular diseases, and neural tube defects [42], their detection is also of great importance.

In this work, the potential application of squaraine dyes derived from 2,3,3-trimethylindolenine and 1,1,2-trimethylbenz[*e*]indole as fluorescent probes for HSA detection is evaluated. The four-membered central ring introduction of diethanolamino, picolyl-, and dipicolylamino groups was studied to understand if these functional groups improve their interaction with this protein compared to unsubstituted squaraines. This work is also comparative with analogous molecules whose albumin interaction results were previously reported in the scope of their potential as photosensitizers for photodynamic therapy (Figure 1) [43]. Thus, four new squaraine dyes similar to those previously reported were

prepared and properly characterized to make this comparative study possible. The absorption of these dyes, emission, and relative fluorescence quantum yields were determined for the prepared dyes in several organic solvents. The interaction of the prepared squaraines with HSA was evaluated *in vitro* by drawing fluorescence spectra at increasing concentrations of this biomolecule. The relative fluorescence quantum yields in the buffer, with and without protein, method sensitivity, and limits of detection and quantification were calculated. Computational studies were performed to determine the sites with which the squaraines have the most significant affinity and the amino acid residues with which they may interact.

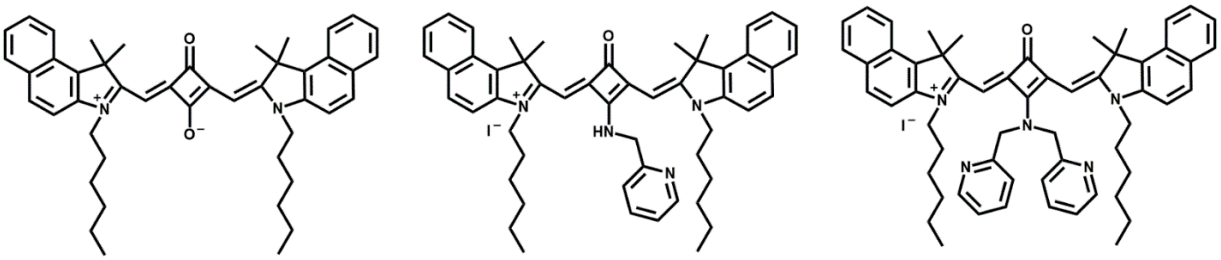

1 **2** **3**

Figure 1. Squaraine dyes **1**–**3**, analog to those prepared in the present work, from which the objective is to make a comparative analysis [43].

2. Materials and Methods

2.1. Instruments and Methods

All reagents and starting materials were of analytical grade and were used as received unless otherwise specified. The dichloromethane used in reactions was previously dried. Reactions under heating and/or magnetic stirring were executed using Velp Scientifica heating magnetic stirrers. The reaction monitoring and assessment of the purity of the synthesized compounds were performed by thin-layer chromatography using Merck 60 F_{254} aluminum sheets coated with 0.25 mm silica gel. After elution in a mixture of 2–10% dichloromethane/methanol, the plates were controlled by the naked eye and, when required, visualized under 254 or 365 nm ultraviolet radiation.

Melting points (M.p.) were determined in a URA Technic hot plate binocular microscope apparatus and are uncorrected. After melting, the residue was eluted in proper solvent and compared chromatographically with the initial crystals to observe if melting led to decomposition. If so, the compounds' characterization describes the abbreviation "dec.". Ground-state visible (Vis) absorption spectra were recorded on a Perkin Elmer Lambda 25 spectrophotometer using an Hellma Analytics 10-mm-path-length two-sided clear quartz cuvette at room temperature with a slit width of 1 nm. Absorbance spectra of the dyes under evaluation were plotted in dimethyl sulfoxide (DMSO), dimethylformamide (DMF), chloroform (CFM), and phosphate buffer (PB). The maximum absorption wavenumbers are described in nm, and the molar absorptivity coefficients, slope of the line plotting the absorbance intensities of five dye's concentration-known solutions versus the sample concentrations, are presented in $M^{-1} \cdot cm^{-1}$. All fluorescence measurements were performed using a Varian Cary Eclipse fluorescence spectrophotometer and an Hellma Analytics 10 mm path length four-sided clear fluorescence/ultraviolet quartz cuvette. Fourier Transform Infrared spectra were measured on a Shimadzu IRAffinity spectrophotometer by means of Shimadzu LabSolutions IR software as KBr pellets. Sample spectra were recorded at room temperature in the range of 4000–500 cm^{-1}, with a spectral resolution of ± 4 cm^{-1}. Bands' wavenumber values (υ_{max}) are described in cm^{-1}, and assignments were made by indicating the strength of the vibration as being of weak (w), medium (m), or strong (s) intensity. The nuclear magnetic resonance of proton (^{1}H NMR) and of carbon-13 (^{13}C NMR) spectra were recorded at 298.15 K in deuterochloroform ($CDCl_3$) or hexadeuterodimethyl sulfoxide (DMSO-d_6) on a Bruker NMR Avance III 400, observing ^{1}H at 400.13 MHz and

^{13}C at 100.63 MHz, or on a Bruker NMR Avance III 600 spectrometer, observing ^{1}H at 600.13 MHz and ^{13}C at 150.90 MHz. Chemical shifts (δ) are reported in parts per million (ppm) relative to tetramethylsilane or residual solvent signals. Coupling constants (*J*) are reported in Hertz. Proton splittings are defined as a singlet (s), broad singlet (br s), doublet (d), broad doublet (br d), triplet (t), broad triplet (br t), double triplet (dt), quintet (qt), or multiplet (m). Carbon-13 assignments were based on distortionless enhancement by polarization transfer 135° (DEPT 135) spectra. High-resolution electrospray ionization time-of-flight mass spectrometry (HRESI-TOFMS) was performed using a microTOF Bruker Daltonics spectrometer at CACTI (University of Vigo).

2.2. Squaraines' Synthesis

2.2.1. 2-{2-[Bis(2-hydroxyethyl)amino]-3-(1-hexyl-3,3-dimethyl-3*H*-indolin-2-ylidenemethyl)-4-oxocyclobut-2-enylidenemethyl}-1-hexyl-3,3-dimethylindol-1-ium iodide (**11a**)

The title compound was obtained by reacting 0.25 g (0.34 mmol) of *O*-methylated squaraine **7a** with 50 μL (0.51 mmol) of diethanolamine (**8**) in dry dichloromethane (25 mL) at room temperature under a nitrogen atmosphere, stirring for 1h. After removing the solvent to dryness on the rotary evaporator, 10 mL of methanol and 10 mL of 14% potassium iodide aqueous solution were added to the resulting residue. The mixture was allowed to stir at room temperature for 2 h. After decanting, the resulting residue was washed with distilled water, crushed with diethyl ether, and dried under vacuum to obtain bright green crystals. Yield: 41%. M.p.: 160–163 °C (dec.). Vis λ_{max} (DMF): 669 nm; Vis λ_{max} (DMSO): 673 nm; Vis λ_{max} (PB): 670 nm; Vis λ_{max} ($CHCl_3$): 667 nm, $\varepsilon = 1.9 \times 10^5$ $M^{-1}\cdot cm^{-1}$. IR υ_{max} (KBr): 3333 (w, OH), 2951 (w, CH), 2924 (w, CH), 2859 (w, CH), 1742 (w, C=O), 1682 (w, C=C), 1539 (w), 1493 (m, ArC=C), 1479 (m), 1454 (m), 1435 (m), 1402 (w), 1360 (w), 1312 (m), 1287 (m), 1234 (w), 1225 (w), 1173 (m), 1105 (m), 1051 (w), 1020 (w), 989 (w), 924 (w), 824 (w), 802 (w), 752 (w), 671 (w) cm^{-1}. ^{1}H NMR (DMSO-d_6, 600 MHz) δ: 7.57 (2H, d, *J* = 7.2, ArH), 7.46 (2H, d, *J* = 7.8, ArH), 7.41 (2H, t, *J* = 7.5, ArH), 7.26 (2H, t, *J* = 7.5, ArH), 6.19 (2H, s, C=C<u>H</u>), 5.31 (2H, t, *J* = 4.8, $N(CH_2)_2O\underline{H}$, exchanges with D_2O), 4.17 (4H, t, *J* = 7.2, $NC\underline{H}_2(CH_2)_4CH_3$), 3.89 (4H, t, *J* = 5.1, $NC\underline{H}_2CH_2OH$), 3.85–3.82 (4H, m, $NCH_2C\underline{H}_2OH$, collapses into a triplet with D_2O), 1.71–1.66 (16H, s + qt, $C(C\underline{H}_3)_2$ + $NCH_2C\underline{H}_2(CH_2)_3CH_3$), 1.35 (4H, qt, *J* = 7.8, $N(CH_2)_2C\underline{H}_2(CH_2)_2CH_3$), 1.28–1.24 (8H, m, $N(CH_2)_3(C\underline{H}_2)_2CH_3$), 0.84 (6H, t, *J* = 6.9, $N(CH_2)_5C\underline{H}_3$) ppm. ^{13}C NMR (DMSO-$d_6$, 150.90 MHz) δ: 174.23, 172.13, 167.91, 158.60, 141.72, 141.62, 128.17 (ArCH), 124.78 (ArCH), 122.30 (ArCH), 111.41 (ArCH), 89.19 (C=<u>C</u>H), 58.58 ($NCH_2\underline{C}H_2OH$), 53.29 ($N\underline{C}H_2CH_2OH$), 49.39 ($\underline{C}(CH_3)_2$), 44.27 ($N\underline{C}H_2(CH_2)_4CH_3$), 30.88 ($CH_2$), 26.71 ($CH_2$), 25.93 ($C(\underline{C}H_3)_2$), 25.69 ($CH_2$), 21.91 ($CH_2$), 13.78 ($CH_3$) ppm. HRESI-TOFMS m/z: 652.4479 $[M–I]^+$ ($C_{42}H_{58}N_3O_3$ calc. 652.4473).

2.2.2. 2-{2-[Bis(2-hydroxyethyl)amino]-3-(3-hexyl-1,1-dimethyl-2*H*-benzo[e]indol-2-ylidenemethyl)-4-oxocyclobut-2-enylidenemethyl}-3-hexyl-1,1-dimethyl-1*H*-benzo[*e*]indol-3-ium iodide (**11b**)

The title compound was obtained by reacting 0.25 g (0.30 mmol) of *O*-methylated squaraine **7b** with 87 μL (0.90 mmol) of diethanolamine (**8**) in dry dichloromethane (25 mL) at room temperature under a nitrogen atmosphere, stirring for 1 h 30 min. After removing the solvent to dryness on the rotary evaporator, 10 mL of methanol and 10 mL of 14% potassium iodide aqueous solution were added to the resulting residue. The mixture was stirred at room temperature for 2 h. After decanting, the resulting residue was washed with distilled water, crushed with diethyl ether, and dried under a vacuum to obtain yellowish-green crystals. Yield: 70%. M.p.: 114–117 °C. Vis λ_{max} (DMF): 703 nm; Vis λ_{max} (DMSO): 707 nm; Vis λ_{max} (PB): 705 nm; Vis λ_{max} ($CHCl_3$): 702 nm, $\varepsilon = 1.7 \times 10^5$ $M^{-1}\cdot cm^{-1}$. IR υ_{max} (KBr): 3335 (w, OH), 2951 (w, CH), 2928 (m, CH), 2857 (w, CH), 1738 (w, C=O), 1622 (m, C=C), 1549 (m, ArC=C), 1520 (w), 1485 (s), 1454 (m), 1433 (m), 1337 (m), 1296 (m), 1246 (m), 1207 (w), 1180 (m), 1117 (m), 1092 (w), 1053 (w), 1015 (w), 986 (w), 934 (m), 891 (w), 806 (m), 746 (w), 671 (m) cm^{-1}. ^{1}H NMR (DMSO-d_6, 600 MHz) δ: 8.28 (2H, d, *J* = 8.4, ArH), 8.08 (2H, d, *J* = 8.4, ArH), 8.06 (2H, d, *J* = 8.4, ArH), 7.80 (2H, d, *J* = 8.4, ArH), 7.65 (2H, t, *J* = 7.8 ArH), 7.51 (2H, t, *J* = 7.5, ArH), 6.26 (2H, s, C=C<u>H</u>), 5.35 (2H,

t, *J* = 5.1, $N(CH_2)_2O\underline{H}$, exchange with D_2O), 4.32 (4H, t, *J* = 7.2, $NC\underline{H}_2(CH_2)_4CH_3$), 3.94 (4H, t, *J* = 5.1, $NC\underline{H}_2CH_2OH$), 3.88–3.86 (4H, m, $NCH_2C\underline{H}_2OH$), 1.93 (12H, s, $C(C\underline{H}_3)_2$), 1.74 (4H, qt, *J* = 7.2, $NCH_2C\underline{H}_2(CH_2)_3CH_3$), 1.38 (4H, qt, *J* = 7.7, $N(CH_2)_2C\underline{H}_2$ $(CH_2)_2CH_3$), 1.31–1.22 (8H, m, $N(CH_2)_3(C\underline{H}_2)_2CH_3$), 0.83 (6H, t, *J* = 6.9, $N(CH_2)_5C\underline{H}_3$) ppm. ^{13}C NMR (DMSO-$d_6$, 150.90 MHz) δ: 174.67, 173.45, 167.81, 157.72, 139.28, 134.10, 131.30, 129.99 (ArCH), 129.74 (ArCH), 127.66 (ArCH), 124.86 (ArCH), 122.53 (ArCH), 111.85 (ArCH), 88.88 (C=$\underline{C}$H), 58.69 ($NCH_2\underline{C}H_2OH$), 53.37 ($N\underline{C}H_2CH_2OH$), 51.12 ($\underline{C}(CH_3)_2$), 44.63 ($N\underline{C}H_2$ $(CH_2)_4CH_3$), 30.93 (CH_2), 27.08 (CH_2), 25.81 ($C(\underline{C}H_3)_2$), 25.68 (CH_2), 21.94 (CH_2), 13.81 (CH_3) ppm. HRESI-TOFMS m/z: 752.4783 $[M–I]^+$ ($C_{50}H_{62}N_3O_3$ calc. 752.4786).

2.2.3. 1-Hexyl-2-[3-(1-hexyl-3,3-dimethyl-3*H*-indolin-2-ylidenemethyl)-4-oxo-2-(pyridin-2-ylmethylamino)cyclobut-2-enylidenemethyl]-3,3-dimethylindol-1-ium iodide (**12a**)

The title compound was obtained by reacting 1.80 g (2.40 mmol) of *O*-methylated squaraine **7a** with 800 μL (7.3 mmol) of 2-picolylamine (**9**) in dry dichloromethane (50 mL) at room temperature under a nitrogen atmosphere, stirring for 4 h. After removing the solvent to dryness on the rotary evaporator, 25 mL of methanol and 25 mL of 14% potassium iodide aqueous solution were added to the resulting residue. The mixture was stirred at room temperature for 2 h. After decanting, the resulting residue, which showed chromatographically to be a complex mixture of several compounds, was washed with distilled water, crushed with diethyl ether, and dried under a vacuum to obtain bright-green crystals. Yield: 12%. M.p.: 203–204 °C (dec.). Vis λ_{max} (DMF): 656 nm; Vis λ_{max} (DMSO): 660 nm; Vis λ_{max} (PB): 657 nm, Vis λ_{max} ($CHCl_3$): 657 nm, $\varepsilon = 3.0 \times 10^5$ $M^{-1}\cdot cm^{-1}$. IR υ_{max} (KBr): 3447 (w, NH), 3092 (w, ArCH), 2955 (m, CH), 2926 (m, CH), 2857 (m, CH), 1632 (s, C=O), 1609 (w, C=C), 1566 (m, ArC=C), 1495 (s), 1462 (s), 1402 (w), 1358 (m), 1294 (m), 1238 (w), 1169 (m), 1130 (w), 1113 (m), 1051 (w), 1020 (w), 924 (w), 833 (m), 797 (w), 748 (m), 673 (w) cm^{-1}. ^{1}H NMR ($CDCl_3$, 600 MHz) δ: 10.10 (1H, br s, NH, exchange with D_2O), 8.52–8.51 (1H, m, ArH), 8.01 (1H, d, *J* = 7.8, ArH), 7.78 (1H, dt, *J* = 7.5, 1.8, ArH), 7.37 (2H, br s, ArH), 7.32 (1H, br s, ArH), 7.24 (1H, br d, *J* = 6.0, ArH), 7.23 (1H, br d, *J* = 5.4, ArH), 7.16 (2H, br s, ArH), 7.00 (1H, br s, ArH), 6.67 (1H, s, C=C$\underline{H}$), 6.22 (1H, s, C=C$\underline{H}$), 5.07 (2H, d, *J* = 6.6, $NHC\underline{H}_2C_5H_4N$), 4.59 (2H, br s, $NC\underline{H}_2(CH_2)_4CH_3$), 4.10 (2H, br s, $NC\underline{H}_2(CH_2)_4CH_3$), 1.86 (2H, br s, $NCH_2C\underline{H}_2(CH_2)_3CH_3$), 1.76 (6H, br s, $C(C\underline{H}_3)_2$), 1.70 (6H, br s, $C(C\underline{H}_3)_2$), 1.55 (2H, br s, $N(CH_2)_2C\underline{H}_2(CH_2)_2CH_3$), 1.37–1.25 (12H, m, $N(CH_2)_2C\underline{H}_2(CH_2)_2CH_3$ + $N(CH_2)_3(C\underline{H}_2)_2CH_3$), 0.85 (6H, t, *J* = 6.9, $N(CH_2)_5C\underline{H}_3$) ppm. ^{1}H NMR ($CDCl_3$ + D_2O, 600 MHz) δ: 8.50 (1H, d, *J* = 4.8, ArH), 8.01 (1H, d, *J* = 7.8, ArH), 7.75 (1H, dt, *J* = 7.5, 1.8, ArH), 7.37 (2H, br t, *J* = 6.0, ArH), 7.32 (1H, d, *J* = 7.2, ArH), 7.31 (1H, t, *J* = 7.2, ArH), 7.24 (1H, t, *J* = 6.6, ArH), 7.23–7.21 (1H, m, ArH), 7.15 (1H, t, *J* = 7.2, ArH), 7.14 (1H, d, *J* = 7.8, ArH), 6.99 (1H, d, *J* = 7.8, ArH), 6.65 (1H, s, C=C$\underline{H}$), 6.22 (1H, s, C=C$\underline{H}$), 5.04 (2H, s, $NHC\underline{H}_2C_5H_4N$), 4.59 (2H, t, *J* = 6.9, $NC\underline{H}_2(CH_2)_4CH_3$), 4.08 (2H, t, *J* = 7.2, $NC\underline{H}_2(CH_2)_4CH_3$), 1.88 (2H, qt, *J* = 7.4, $NCH_2C\underline{H}_2(CH_2)_3CH_3$), 1.75 (6H, s, $C(C\underline{H}_3)_2$), 1.72–1.69 (8H, s + m, $C(C\underline{H}_3)_2$ + $NCH_2C\underline{H}_2(CH_2)_3CH_3$), 1,55 (2H, qt, *J* = 8.0, $N(CH_2)_2C\underline{H}_2(CH_2)_2CH_3$), 1.37–1.24 (10H, m, $NCH_2(C\underline{H}_2)_3CH_3$ + $N(CH_2)_3(C\underline{H}_2)_2CH_3$), 0.84 (6H, br t, *J* = 6.6, $N(CH_2)_5C\underline{H}_3$) ppm. ^{13}C NMR ($CDCl_3$, 150.90 MHz) δ: 174.27, 173.57, 171.04, 168.76, 162.16, 157.84, 148.16 (ArCH), 142.93, 142.08, 141.97, 141.79, 137.75 (ArCH), 128.10 (ArCH), 127.87 (ArCH), 125.35 (ArCH), 124.26 (ArCH), 124.05, 122.89 (ArCH), 122.09 (ArCH), 111.22 (ArCH), 109.80 (ArCH), 90.80 (C=$\underline{C}$H), 88.92 (C=$\underline{C}$H), 50.03 ($\underline{C}(CH_3)_2$), 49.21 ($\underline{C}(CH_3)_2$), 48.27 ($NH\underline{C}H_2C_5H_4N$), 45.22 ($N\underline{C}H_2(CH_2)_4CH_3$), 43.81 ($N\underline{C}H_2(CH_2)_4CH_3$), 31.55 ($CH_2$), 31.48 ($CH_2$), 27.80 ($CH_2$), 27.15 ($CH_2$), 26.73 ($C(\underline{C}H_3)_2$), 26.34 ($CH_2$), 26.06 ($C(\underline{C}H_3)_2$), 22.35 ($CH_2$), 13.95 ($CH_3$), 13.88 ($CH_3$) ppm. HRESI-TOFMS m/z: 655.4374 $[M–I]^+$ ($C_{44}H_{55}N_4O$ calc. 655.4370).

2.2.4. 2-[2-Bis(pyridin-2-ylmethyl)amino-3-(1-hexyl-3,3-dimethyl-3*H*-indolin-2-ylidenemethyl)-4-oxocyclobut-2-enylidenemethyl]-1-hexyl-3,3-dimethylindol-1-ium iodide (**13a**)

The title compound was obtained by reacting 0.25 g (0.34 mmol) of *O*-methylated squaraine **7a** with 245 μL (1.4 mmol) of di-(2-picolyl)amine (**10**) in dry dichloromethane (50 mL) at room temperature under a nitrogen atmosphere, stirring for 24 h. After removing

the solvent to dryness on the rotary evaporator, 5 mL of methanol and 5 mL of 14% potassium iodide aqueous solution were added to the resulting residue. The mixture was stirred at room temperature for 1 h. After decanting, the resulting residue was washed several times with distilled water, crushed with diethyl ether and petroleum ether, and dried under vacuum to obtain dark violet crystals. Yield: 37%. M.p.: 82–84 °C. Vis λ_{max} (DMF): 665 nm; Vis λ_{max} (DMSO): 668 nm; Vis λ_{max} (PB): 665 nm; Vis λ_{max} ($CHCl_3$): 664 nm, $\varepsilon = 1.5 \times 10^5\ M^{-1}{\cdot}cm^{-1}$. IR υ_{max} (KBr): 3048 (w, ArCH), 2953 (m, CH), 2826 (m, CH), 2857 (w, CH), 1744 (w, C=O), 1626 (w, C=C), 1543 (m, ArC=C), 1491 (s, ArC=C), 1479 (s), 1454 (s), 1435 (s), 1361 (m), 1312 (s), 1287 (s), 1238 (w), 1223 (w), 1175 (m), 1128 (w), 1105 (s), 1049 (w), 1020 (w), 984 (w), 922 (w), 754 (w), 681 (w) cm^{-1}; ^{1}H NMR (DMSO-d_6, 400 MHz) δ: 8.66 (2H, br s, ArH), 7.87 (2H, br t, *J* = 6.6, ArH), 7.56 (4H, d, *J* = 6.4, ArH), 7.43–7.35 (6H, m, ArH), 7.25 (2H, br s, ArH), 5.99 (2H, s, C=C$\underline{H}$), 5.16 (4H, s, NC$\underline{H}_2C_5H_4N$), 3.85 (4H, br t, *J* = 6.2, NC$\underline{H}_2(CH_2)_4CH_3$), 1.63 (12H, s, C(C$\underline{H}_3)_2$), 1.32 (4H, qt, *J* = 7.3, $NCH_2C\underline{H}_2(CH_2)_3CH_3$), 1,16–1,05 (8H, m, $N(CH_2)_3(C\underline{H}_2)_2CH_3$), 0.95 (4H, qt, *J* = 7.2, $N(CH_2)_2C\underline{H}_2(CH_2)_2CH_3$), 0.77 (6H, br t, *J* = 6.2, $N(CH_2)_5C\underline{H}_3$) ppm. ^{13}C NMR (DMSO-$d_6$, 150.90 MHz) δ: 173.88, 171.70, 168.05, 158.27, 154.48, 149.14 (ArCH), 141.07, 140.93, 136.77 (ArCH), 127.56 (ArCH), 124.31 (ArCH), 122.61 (ArCH), 121.95 (ArCH), 121.67 (ArCH), 110.82 (ArCH), 88.13 (C=$\underline{C}$H), 56.03 ($N(\underline{C}H_2C_5H_4N)_2$), 48.86 ($\underline{C}(CH_3)_2$), 43.45 ($N\underline{C}H_2(CH_2)_4CH_3$), 30.10 ($CH_2$), 25.87 ($CH_2$), 25.28 (C($\underline{C}H_3$)), 24.84 ($CH_2$), 21.19 ($CH_2$), 13.08 ($CH_3$) ppm. HRESI-TOFMS m/z: 746.4784 $[M–I]^+$ ($C_{50}H_{60}N_5O$ calc. 746.4792).

2.3. Fluorescence Measurements

Squaraine dyes' stock solutions were prepared at 6.7×10^{-4} M, dissolving each dye in analytical-grade DMF. Human serum protein stock solution was prepared at 14.0×10^{-4} M in PB (0.05 M, pH 7.4). All fluorometric measurements were performed in triplicate.

2.3.1. Relative Fluorescence Quantum Yields Calculations

Relative fluorescence quantum yields (Φ_F) were determined by the comparison of the integrated spectra area of each squaraine dye with the zinc phthalocyanine standard reference area, with a quantum yield for DMF of 0.17 and DMSO of 0.20, using the following equation (Equation (1); [44]):

$$\Phi_F = \Phi_{F\ (Std)} \left(\frac{Grad_{SqD}}{Grad_{Std}} \right) \left(\frac{\eta^2_{SqD}}{\eta^2_{Std}} \right) \quad (1)$$

where the subscripts "Std" and "SqD" refer to standard and squaraine dye, respectively, "Grad" to the gradient from the plot-integrated fluorescence versus absorbance, and "η" to the refractive index of the solvent. Fluorescence spectra were displayed, exciting the compounds in varying wavelengths according to the absorption spectra of the squaraine dye in the organic solvent under study, with an excitation and emission slit width of 5 nm. The emission spectra areas of the standard dye and the squaraine dye were obtained using fluorometric measurements at the same excitation wavelength and slit width.

2.3.2. Squaraine–Protein Interaction Evaluation

Due to the insoluble character of squaraine dyes in aqueous media, compounds' solutions for the protein–dye interaction assays were prepared in DMF and then diluted in PB. To this solution, HSA protein stock solution was added, where the squaraine concentrations were maintained (2.0 μM), and the protein concentrations varied from 0 to 3.0 μM (0, 0.05, 0.1, 0.2, 0.4, 0.6, 0.8, 1.0, 1.5, 2.0, 3.0 μM). The fluorescence intensity of the final solutions was read at t = 0, 1, 2, and 3 h of incubation with the protein, using the excitation wavelength and excitation and emission slit widths depending on each dye (Table 1). The excitation wavelength of each dye was adjusted concerning their maximum absorption since the Stokes shifts are not large enough for us to be able to excite them to the maximum absorption values.

Table 1. Excitation wavelength and excitation/emission slit width values used for squaraine–protein binding fluorescence intensity measurements.

Squaraine Dye	Excitation Wavelength (nm)	Excitation/Emission Slits (nm)
5a	590	5/10
11a	630	10/10
11b	670	10/10
12a	595	10/10
13a	620	10/10

In both the absence and presence of proteins, relative fluorescence quantum yields were calculated as indicated in Section 2.3.1. In the latter case, the emission spectra at the maximum HSA concentration were used.

To prove the potential sensors' selectivity, squaraines' interaction spectra with human gamma globulin (γ-globulin) proteins were displayed at the highest protein concentration tested (3.0 μM), using the same excitation wavelengths and the same slit widths and compared with those obtained at the same serum albumin concentration.

Detection and Quantification Limits Calculation

Detection and quantification limits (DL and QL, respectively), the lowest concentration of an analyte that can be consistently detected and the lowest level of an analyte that can be quantified with any degree of certainty [45], respectively, were calculated from a calibration line plotting the maximum fluorescence intensity versus the concentrations of protein. From the slope of this line, or method sensitivity, Equations (2) and (3) were applied:

$$DL = \frac{3\sigma}{S} \quad (2)$$

$$QL = \frac{10\sigma}{S} \quad (3)$$

where σ refers to the blank standard deviation, and S (sensitivity) to the linear regression slope between the fluorescence intensity and albumin concentration.

2.4. Computational Studies

AutoDock Tools (autodock4.exe) 1.5.6 software (The Scripps Research Institute) was used to dock squaraine dyes **5a**, **11a**,**b**, **12a**, and **13a** with HSA in Sudlow sites I and II and considering the whole protein. Under the codes 2BXD and 2BXG, the crystal structures of HSA were retrieved from the Research Collaboratory for Structural Bioinformatics Protein Data Bank [RCSB PDB, http://www.rscb.org (accessed on 26 April 2022)] with *R*-warfarin and ibuprofen as co-crystallized ligands in the Sudlow site I (2BXD) and Sudlow site II (2BXG) crystal structures of HSA, respectively. The University of California San Francisco (UCSF) Chimera 1.13.1 software was used to prepare and isolate proteins and their co-crystallized ligands, with the chain B and water of the complex ligand–protein removed. Squaraines were sketched in ChemDraw software, queued into Chem3D for energy minimization to the lowest energy conformation at a Minimum RMS Gradient of 0.01, and exported in a ".mol2" format. The PDBQT file of the dyes was created using OpenBabel 3.1.1 from the ".mol2" format.

All hydrogen atoms were added to the protein structure, Gasteiger charges were computed, non-polar hydrogens were merged, and AD4-type atoms were allocated to the protein structure in ADT.

The coordinates (x, y, z) 3.376, (−9.600), 5.600, and the size (x, y, z) of 60 × 60 × 60 points with 0.375 spacing, were used to define the Grid Box for 2BXD. The coordinates (x, y, z) in 2BXG were 5.048, (−4.464), (−15.042), with a size (x, y, z) of 60 × 90 × 50 points and a spacing of 0.375. The Grid Box center was defined as the center of the macromolecule

with the coordinates (x, y, z) −0.16, −0.696, 0.101 and the size of 90 × 126 × 102 (x, y, z) points with 0.800 spacing in the docking, considering all proteins using 2BXD. Docking was performed using the Lamarckian genetic algorithm (GA) with 60 GA runs, a 150 GA population size, a maximum number of generations of 27,000, a maximum number of energies evals of 5,000,000, and a maximum number of top individuals surviving to the next generation of 1. The conformation of each squaraine dye and co-crystallized protein ligand with the lowest estimated free binding energy (BE in Kcal/mol) was chosen and selected for the analysis of the ligand–protein interactions by means of Discovery Studio 2016 software.

The water solubility (WS) of squaraines dyes **5a**, **11a**,**b**, **12a**, and **13a** was predicted using the pkCSM tool [46] and is presented in log (mol/L).

3. Results

3.1. Chemistry

The synthetic strategy used to obtain the desired squaraine dyes **5a**, **11a**,**b**, **12a**, and **13a** (Scheme 1) was similar to that recently reported [47–49]. Briefly, after the *N*-alkylation reaction of heterocycles **1a** and **1b** with iodohexane (**2**) and their condensation with squaric acid (**4**), corresponding zwitterionic dyes **5a** and **5b** were obtained. The latter were methylated with an excess of methyl trifluoromethanesulfonate (**6**; $CF_3SO_3CH_3$) at room temperature under a nitrogen atmosphere, obtaining the corresponding *O*-methyl ethers **7a** and **7b**. By reacting these *O*-methyl ether derivatives with several amines, such as diethanolamine (**8**), 2-picolylamine (**9**), and di-(2-picolyl)amine (**10**), the triflate-counterioned aminosquaraine dyes **11a**,**b**, **12a**, and **13a** were obtained, and then subjected to the counterion exchange to iodide after treatment with 14% potassium iodide aqueous solution.

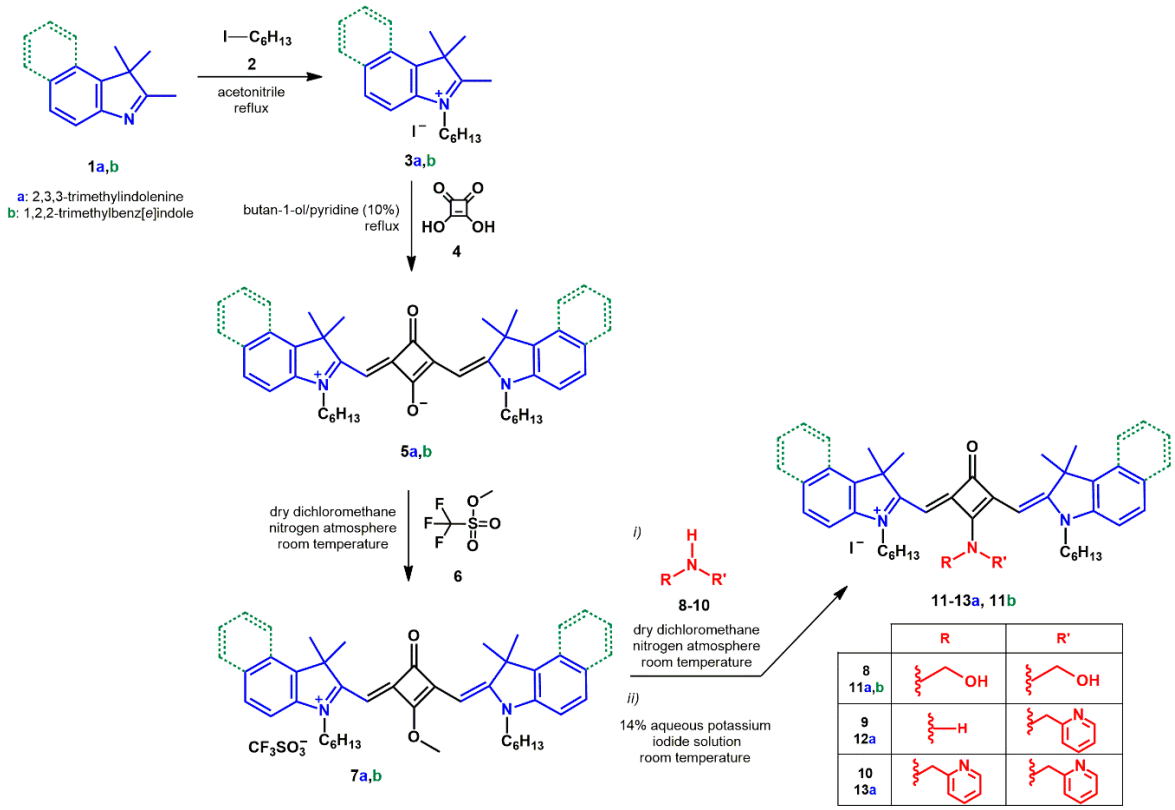

Scheme 1. Synthetic approach for synthesizing the desired squaraine dyes **5a**, **11a**,**b**, **12a**, and **13a**.

^{1}H and ^{13}C NMR spectra are included as supplementary material (Figures S1–S11) and are in agreement with what is expected for this kind of compounds [50,51]. The authors emphasize the spectra of compound **12a** that show the typical signals of an asymmetric

squaraine, in particular, the chemical shifts of methine protons in the ^{1}H NMR spectrum at 6.67 and 6.22 ppm and the corresponding carbons in the ^{13}C NMR spectrum at 90.80 and 88.92 ppm.

3.2. Photophysical Properties

Visible absorption is an important parameter in the spectroscopic characterization of the prepared squaraine dyes since, to be considered suitable fluorescent probes, these molecules must exhibit high absorption and emission wavelengths (650–900 nm) to minimize interference caused by the biological samples' fluorescence [52,53].

Through the visible spectra of squaraine dyes **5a**, **11a**,**b**, **12a**, and **13a**, it is observable that they present maximum absorption peaks in DMF between 642 and 703 nm, in DMSO between 645 and 707 nm, and in CFM between 636 and 702 nm (Table 2 and Figure S12). The absorption behavior of the dyes did not vary significantly in the three organic solvents studied, with a near overlap of these same absorption spectra being observed. In CFM, all squaraines exhibited very high molar absorptivity coefficients (ε = 1.48–3.98 × 10^5 M^{-1}·cm^{-1}), demonstrating their ability to absorb radiation for a subsequent release of energy presented as fluorescence emission. In addition, moderate Stokes shifts were observed (ΔS = 245–369 cm^{-1}). In organic solvents, squaraine dye **5a** was the most fluorescent, with quantum yields from 21.1% in DMF to greater than 100% in CFM. This quantum yield of fluorescence slightly above 100% is due to the fact that it was calculated by a comparative method as well as the errors associated with the experimental approach. Therefore, this value should be analyzed carefully since it only indicates that for approximately every 100 photons absorbed, 100 were emitted. Marked differences in the quantum yields of fluorescence of the squaraine **5a** in the evaluated solvents are mainly due to its nonpolar nature; therefore, it exhibits higher quantum yields in solvents of a more lipophilic nature (chloroform) than in more hydrophilic ones (dimethylformamide and dimethyl sulfoxide). Ethanolamine- and picolylamine-bearing squaraine dyes **11a**,**b**, **12a**, and **13a** showed considerably lower relative quantum yields (Φ_F = 1.7–10.7%). Given their poor emission ability in these organic solvents, these latter dyes have had normalized emission spectra with poor resolutions.

Table 2. Maximum absorption and emission wavelengths (λ_{abs} and λ_{em}, respectively; in nm), Stokes shift (ΔS; cm^{-1}), and relative fluorescence quantum yields [Φ_F; in percentage (%)] of squaraine dyes **5a**, **11a**,**b**, **12a**, and **13a** in dimethylformamide (DMF), dimethyl sulfoxide (DMSO), and chloroform (CFM).

		Squaraine Dyes				
Solvent		**5a**	**11a**	**11b**	**12a**	**13a**
DMF	λ_{abs}	642	670	703	656	665
	λ_{em}	655	687	718	671	677
	ΔS	309	369	297	341	267
	Φ_F	21.1 ± 0.3	3.6 ± 0.2	1.7 ± 0.3	5.5 ± 0.4	5.4 ± 0.4
DMSO	λ_{abs}	645	673	707	660	668
	λ_{em}	658	685	725	674	680
	ΔS	306	260	351	315	264
	Φ_F	58.9 ± 2.7	4.1 ± 0.3	2.3 ± 0.4	8.3 ± 0.6	7.1 ± 0.1
CFM	λ_{abs}	636	667	702	657	664
	ε	3.98	1.94	1.67	3.02	1.48
	λ_{em}	650	681	715	671	675
	ΔS	339	308	259	317	245
	Φ_F	116.1 ± 10.4	2.7 ± 0.1	2.3 ± 0.3	10.7 ± 0.9	1.9 ± 0.1

3.3. Squaraine–Protein Interaction Studies

To evaluate the HSA detection ability of each prepared squaraine dye, solutions of dyes in PB were used, keeping their concentration constant (2.0 μM), and then increasing

concentrations of protein (0.0 to 3.0 μM) were added. The fluorescence intensity of the prepared protein–dye solutions was fluorometrically read after an incubation time (0 min, 1, 2 and 3 h) to observe when a complete interaction with the protein, and consequently the maximum fluorescence intensity, is reached.

Figure 2 shows the emission spectra of the squaraines under evaluation in PB and after the successive addition of concentration-increasing HSA solutions, as well as the respective plots that represent the linearity between the concentration of HSA and the fluorescence intensity of the squaraine–protein solutions obtained from at the wavelength of maximum emission. From these spectra, it is possible to verify that all dyes interacted with the protein since there is an increase in fluorescence intensity with increasing HSA concentrations. The linearity between the fluorescence intensity and the HSA concentration is also noticeable through the lines obtained with correlation coefficients (r^2) between 0.9 and 1.0. For squaraine dyes **12a** and **13a**, the maximum fluorescence intensity was observed immediately after adding the protein to the respective dye solution in the buffer. For squaraine dyes **5a**, **11a**, and **11b**, the highest fluorescence intensity was observed after one incubation hour. This analysis is completed by observing the linear regression graphs shown in Figure 2, in which the linear regressions with steeper slopes correspond to the time at which the dye showed a more robust interaction with the protein.

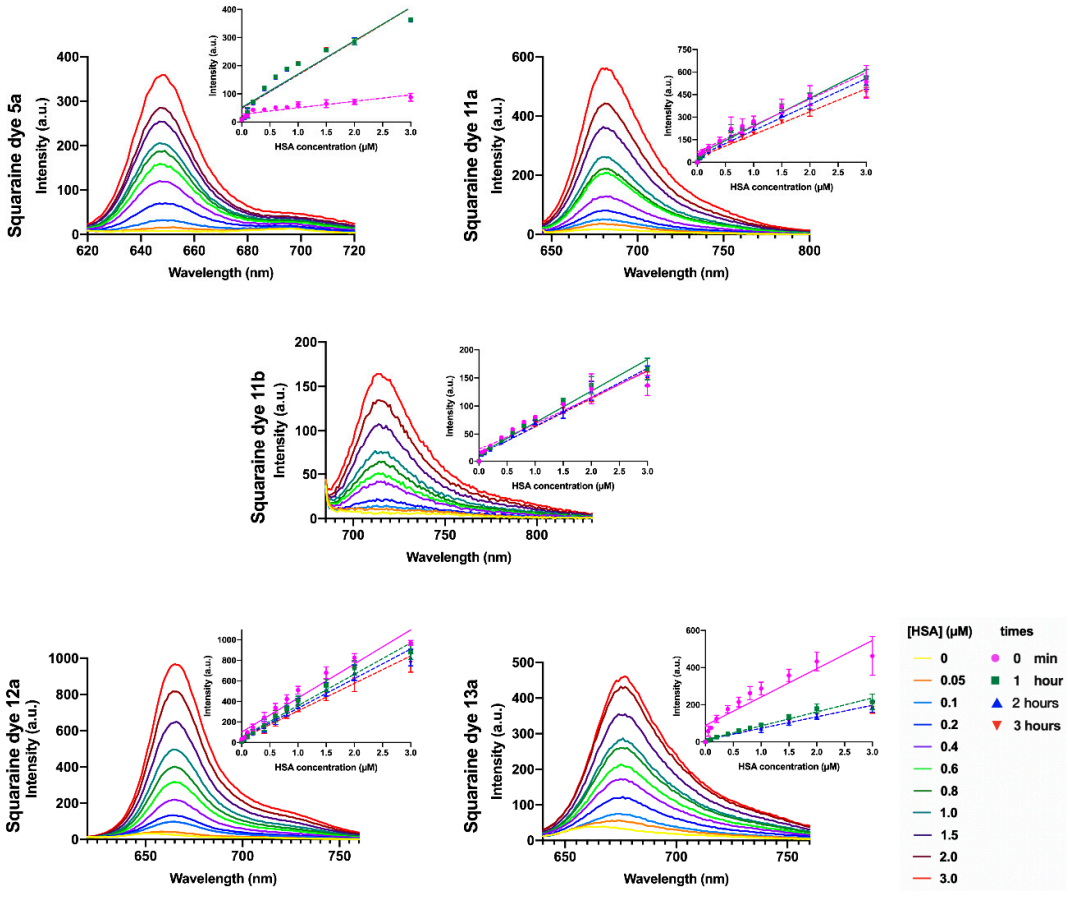

Figure 2. Fluorescence spectra of the squaraine dyes (**5a**, **11a**,**b**, **12a**, and **13a**) on phosphate buffer pH 7.4, with increasing concentrations of human serum albumin (0.00, 0.05, 0.10, 0.20, 0.40, 0.60, 0.80, 1.00, 1.50, 2.00 and 3.00 μM) and regression plots of the emitted fluorescence intensity as a function of protein concentration at various incubation times (t = 0, 1, 2 and 3 h). Data on the plots are the mean ± standard deviation of three independent assays. Spectra presented correspond to the time in which the dye exhibited more expressive fluorescence intensity in the shortest required time (full line). Fluorescence intensity is presented as arbitrary units (a.u.).

In the literature, it is already well described that squaraines in buffer solution with an absence of protein exhibit a very low fluorescence intensity (close to zero) due to the formation of non-fluorescent aggregates [54–56]. Similarly, all evaluated squaraines showed a very low fluorescence intensity and quantum yields in protein-free buffer (Figure 2 and Table 3). Interestingly, picolylamine-bearing dyes **12a** and **13a** exhibited fluorescence intensities in the order of 29 and 38 arbitrary units in the absence of protein, values considerably higher than those usually observed, even compared to the other dyes herein evaluated (Table 4). Of the evaluated squaraines, the zwitterionic **5a** was the one that showed the greatest interaction with the protein in the fluorescence assays, with an F/F_0 ratio of 41 times. Dyes **11a**,**b** and **12a** also showed interaction with serum albumin, with the order of interaction being **12a** > **11a** > **11b**. Squaraine **13a** was also shown to increase its fluorescence in samples with albumin, albeit with an F/F_0 ratio of 12, markedly lower than the other compounds.

Table 3. Differences observed in the absorption and fluorescence properties of squaraine dyes **5a**, **11a**,**b**, **12a**, and **13a** in phosphate buffer in the absence and presence of human serum albumin (HSA). The maximum absorption and emission wavelengths (λ_{abs} and λ_{em}, respectively), as well as the Stokes shift (ΔS), are given in cm^{-1}, the molar absorptivity coefficients (ε) are shown in $\times 10^5$ $M^{-1} \cdot cm^{-1}$, and the relative fluorescence quantum yields (Φ_F) are given in percentages.

Squaraine Dye	HSA Absence					HSA Presence			
	λ_{abs}	λ_{em}	ΔS	ε	Φ_F	λ_{abs}	λ_{em}	ΔS	Φ_F
5a	640	649	217	0.81	1.0 ± 0.1	640	648	193	27.3 ± 0.3
11a	670	680	219	0.48	4.7 ± 0.9	667	682	330	80.1 ± 7.7
11b	705	715	198	0.44	1.9 ± 0.5	707	714	108	28.8 ± 6.3
12a	657	665	182	0.71	3.5 ± 1.0	656	665	206	74.9 ± 3.0
13a	665	675	223	0.23	19.4 ± 3.3	663	677	312	93.2 ± 22.0

Table 4. Determined squaraine–albumin interaction fluorescence of squaraine dyes **5a**, **11a**,**b**, **12a**, and **13a** [fluorescence intensity in the absence of protein (F_0), squaraine fluorescence intensity observed at the highest concentration of protein (F), ratio between these last two parameters (F/F_0), sensitivity (S), and quantification and detection limits (QL and DL, respectively)]. Predicted water solubility (WS) of squaraine dyes is given in log (mol/L).

Squaraine Dye	WS	F_0 (a.u.)	Squaraine-Protein Complex Fluorescence Properties				
			F (a.u.)	F/F_0	S (nM)	QL (nM)	DL (nM)
5a	−5.91	9	363	41	1.0×10^5	1047	314
11a	−4.75	19	564	31	2.0×10^5	635	190
11b	−3.54	8	166	21	5.5×10^5	560	168
12a	−4.99	29	968	36	3.0×10^5	692	208
13a	−4.52	38	463	12	1.0×10^5	1172	352

Compared to CFM, the molar absorptivity coefficients of the squaraines were much more reduced in PB (Table 3). The presence of the protein has not been shown to change the absorption and emission wavelengths of the squaraines. As expected, according to the results shown in Figure 2, very high relative fluorescence quantum yields (Φ_F = 27.3–93.2%) were observed when incubated with the HSA, again proving the dye–protein interaction. Quantum yields with higher standard deviations, such as for squaraine dye **13a** in the presence of albumin, are justified by the high sensitivity of the protein–dye complex to external factors such as, for example, small fluctuations in the temperature at which the measurements were performed. Furthermore, the relative fluorescence quantum yields of squaraines **11a**,**b**, **12a**, and **13a** in HSA-containing buffer proved even higher than those calculated in organic solvents.

From the fluorescence data obtained previously, the detection limit, quantification limit, and method sensitivity parameters were calculated for each squaraine dye. The squaraine dyes that exhibited the lowest detection limits were **11a** and **11b** (DL = 190 and 168 nM, respectively). Consequently, they were also the ones that also exhibited the lowest quantification limits (QL = 635 and 560 nM, respectively). Proportionally, although compounds **5a** and **13a** showed higher detection limits, the quantification limits are markedly higher than the other dyes. The binding affinity was too weak to observe saturation in the evaluated protein concentration range.

Regarding the sensitivity of squaraine dyes as potential fluorescent probes, the method is more sensitive the higher the fluorescence variation at the lowest protein concentration. Squaraines **11a**,**b** and **12a** were the ones that caused the most significant increase in fluorescence intensity at the lowest protein concentration, so these are the ones with the most considerable sensitivity (S = 2.0×10^5, 5.5×10^5, and 3.0×10^5 nM, respectively). The application of the method using the remaining dyes showed lower sensitivity, but in the same order of magnitude ($\times 10^5$ nM).

As the adequate solubility of a protein sensor in aqueous media is essential, this squaraines' property was predicted, showing oscillations depending on the structural changes carried out (Table 4). The unsubstituted squaraine dye **5a** showed the worst solubility in water, which was expected since the introduction of amines modulates the lipophilicity of this class of compounds, increasing its polarity. According to the solubility categories provided by pkCSM, the introduction of the amines made the squaraines moderately soluble in water. On the other hand, the diethanolamine-bearing benz[*e*]indole-based squaraine **11b** was the one that proved to exhibit more excellent solubility in water, as it presented the WS value closer to 0. Strategies that could significantly improve the solubility of these compounds would be reducing the carbon number of the *N*-alkyl chains and introducing groups that increase their polarity, such as primary and secondary amines and hydroxyl groups or carboxylic acids. Functionalizing the side chains with sultones, phosphoryl groups, and other charged groups are alternatives to modulate the squaraines' hydro- and lipophilicity and markedly improve their biocompatibility.

Gamma globulins are the most abundant class of serum proteins after albumin. Given their high presence in serum, the study of selective fluorescence intensity increases for HSA compared to the presence of γ-globulins is of significant relevance. For this purpose, the squaraine–globulin fluorescence spectra were displayed at the highest protein concentration tested (3.0 μM) and compared with those obtained at the same serum albumin concentration to demonstrate the selectivity of the potential sensors. All dyes exhibited higher fluorescence intensities in the presence of albumin than γ-globulins, indicating a better interaction with HSA (Figure 3 and Figure S13). Despite this, for example, squaraine dye **11b** was the one that showed the lowest selectivity, showing fluorescence intensities about three times higher when incubated with HSA. Squaraine dye **12a** showed the most remarkable difference between the intensity emitted in the presence of albumin and γ-globulins, showing a fluorescence intensity about fifteen times lower in the presence of globulins. Compared with the fluorescence emitted by the squaraines alone in buffer, the fluorescence observed when incubated with the globulins was not markedly superior, regardless of the dye under study.

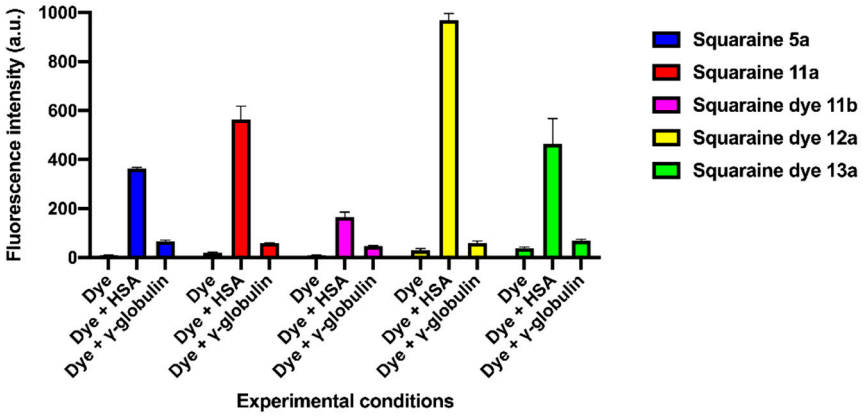

Figure 3. Graph for comparison of the fluorescence intensity maximum to the maximum emission wavelength of squaraine dyes **5a**, **11a**,**b**, **12a**, and **13a** in phosphate buffer pH 7.4 at a concentration of 2.0 μM in the presence and absence of human γ-globulin and serum albumin proteins at a concentration of 3.0 μM. Fluorescence intensities were obtained at the incubation time with the highest albumin–dye interaction and are presented as arbitrary units (a.u.).

3.4. In Silico Studies

Human serum albumin contains three homologous α-helical domains I-III, each separated into subdomains A and B. It is involved in the transport of both drugs (e.g., warfarin) and endogenous ligands (e.g., fatty acids, bilirubin, heme group) in the bloodstream [57]. There are several known binding sites for their interaction with various drugs, with Sudlow sites I and II being the most frequently studied [57–59]. As a result, molecular docking of the squaraine dyes **5a**, **11a**,**b**, **12a**, and **13a** with HSA was carried out in Sudlow sites I (PDB code: 2BXD) and II (PDB code: 2BXG) [58]. Additionally, the co-crystallized ligands (warfarin and ibuprofen from Sudlow site I and II, respectively) were docked, and the results were consistent with previous studies (Tables S1 and S2), validating docking parameters [59,60].

3.4.1. Interaction with Sudlow Site I

Sudlow site I is the binding site for warfarin, a thrombolytic agent. The pocket interior wall consists of hydrophobic side chains, while the entrance is positively charged due to LYS195, LYS199, ARG218, ARG222, HIS242, and ARG257. TYR150, PHE211, TRP214, ALA215, LEU238, and ILE264 are among the residues remaining in Sudlow site I [57,58,60]. According to Table 5, warfarin interacts with most of these amino acid residues, with an estimated BE of −8.79 Kcal/mol. Warfarin forms hydrogen bonds (H-bonds) with TYR150, ARG222, HIS242, and ARG257, and electrostatic interactions with the residue LYS199. LYS195, TRP214, ALA215, ARG218, LEU219, and LEU238 exhibited hydrophobic interactions (Figure 4 and Table S1).

Table 5. Estimated free binding energy of warfarin, ibuprofen, and squaraine dyes **5a**, **11a**,**b**, **12a**, and **13a** in Sudlow sites I and II and full human serum albumin (HSA).

Ligand	Estimated Free Binding Energy (Kcal/mol)						
	Warfarin	**Ibuprofen**	**5a**	**11a**	**11b**	**12a**	**13a**
Protein 2BXD Sudlow Site I	−8.80	–	−12.08	−11.07	−12.15	−13.12	−12.34
Protein 2BXG Sudlow Site II	–	−7.42	−8.36	−8.83	−10.21	−8.87	−9.41
Protein 2BXG Full Protein	–	–	−9.09	−6.84	−9.67	−8.66	−9.25

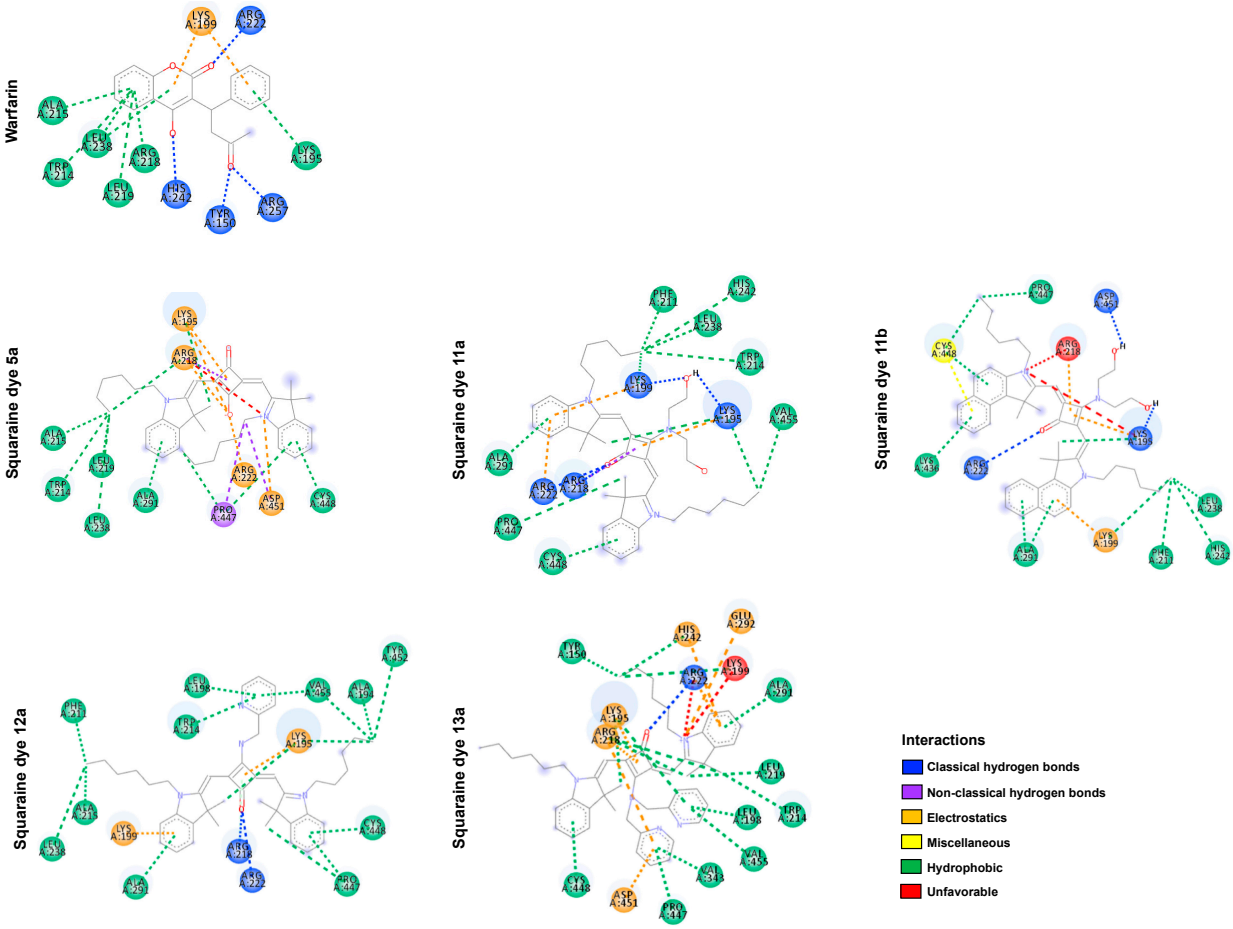

Figure 4. Binding modes and interactions of warfarin and squaraine dyes **5a**, **11a**,**b**, **12a**, and **13a** with amino acid residues of human serum albumin protein at Sudlow site I.

Regarding the squaraine dyes, all revealed BE values lower than warfarin, indicating that the prepared dyes could be suitable substrates of HSA. Picolylamine-bearing squaraine dye **13a** was the best ligand with a BE of −13.12 Kcal/mol (Table 5). The dyes that showed more hydrophobic interactions had a greater affinity to this active site. Squaraine dyes **5a**, **11b**, and **13a** demonstrated charge repulsion interactions.

3.4.2. Interaction with Sudlow Site II

Sudlow site II is mainly constituted of hydrophobic side chains and some disulfide bridges with ARG410 placed at the pocket entrance with TYR411, which has a hydroxyl group facing towards the inside. In addition, the amino acid residues ARG348, GLU383, LYS414, VAL433, GLU450, ARG485, and SER489 are also present in this pocket [57,58,60].

Figure 5 shows that ibuprofen interacts with most of these amino acid residues, mainly through hydrophobic interactions. H-bonds were observed with ARG410 and TYR 411. The BE of the best conformation was −7.42 Kcal/mol (Table 5). All evaluated squaraine dyes demonstrated more proficient binding to this receptor than the co-crystallized ligand in Sudlow site II. In comparison, the interaction with this site was lower than that with Sudlow site I. The majority of the interactions of dyes were hydrophobic (Figure 5 and Table S2). On this site, only a few electrostatic interactions were observed. Squaraine dye **11b**, which demonstrated more H-bonds and electrostatic interactions, was the best ligand among the tested dyes (BE = −10.21 Kcal/mol).

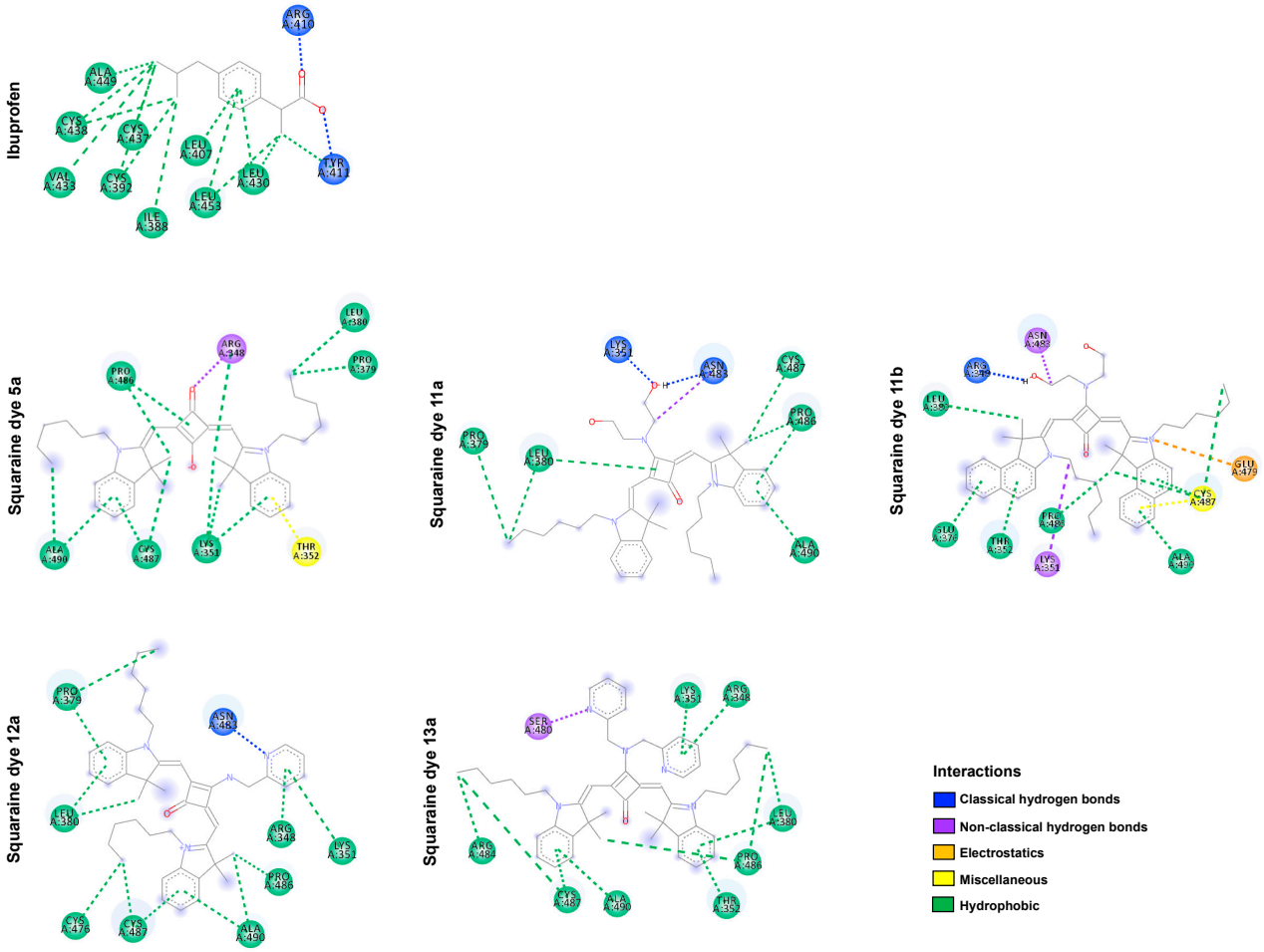

Figure 5. Binding modes and interactions of ibuprofen and squaraine dyes **5a**, **11a**,**b**, **12a**, and **13a** with amino acid residues of human serum albumin protein at Sudlow site II.

3.4.3. Docking with the Full Protein

Due to all the substrates of HSA and the several ligands of this transporter protein, molecular docking was performed considering the whole protein [57–60]. This simulation demonstrated squaraine **11b** as having the best binding affinity to the HSA with a BE of −9.67 Kcal/mol (Table 5). The interactions observed are present in Table S3 and Figure S14.

4. Discussion

Based on the noteworthy results previously reported using squaraine dyes derived from benz[*e*]indole (**1**–**3**; Figure 1) with a view to being used as photosensitizers for photodynamic therapy [43], five squaraine dyes analogous to these were prepared in order to better understand the role of structural modifications in this core of compounds in its interaction with the HSA protein. Furthermore, in addition to the picolyl- and dipicolylamine groups that had already been recently considered, the introduction of the diethanolamine group was studied to provide better hydrophilicity to the compounds due to the hydroxyl groups present in them, improving their suitability for biological experiments.

Despite the low relative fluorescence quantum yields observed in PB, the dyes showed the ability to fluoresce after incubation with albumin. The fluorescence emitted by all squaraines was directly proportional to the protein concentration. The ideal incubation time for displaying the highest possible intensity varied according to the dye under study: while those loaded with picolyl- and dipicolylamino groups exhibited maximum fluorescence at t = 0, the remaining compounds required 1 h of incubation. However, this rapid interaction with the protein is not necessarily related to the picolyl- and dipicolylamino groups since

squaraine **2**, also loaded with the group with a single pyridine unit, required 3 h of incubation to exhibit maximum fluorescence [43]. The fact that the structure of dyes affects the response time had already been reported by Barbero et al., who found that the heterocyclic unit of indolenine, due to its smaller dimension, compared to the bulkier benz[*e*]indole-based derivatives, aimed at a faster and more effective interaction [2]. This last theory should be the explanatory basis for the results achieved. Furthermore, evidence shows that, after some time, the dye may again dissociate from albumin since a straight fluorescence intensity versus a protein concentration with lower slopes is obtained after enhanced interaction (more evident for squaraine **13a**, which exhibits fluorescence intensity versus protein concentrations plots with decreased slopes after 1 and 2 h of incubation compared to t = 0).

At the time at which the fluorescence emitted by the protein–dye adducts is more evident and at the highest protein concentration tested, high quantum yields of fluorescence were obtained (Φ_F = 27.3–93.2%), highlighting that for dye **13a**. However, this fact does not directly indicate a better interaction since squaraine **13a** presents the highest relative fluorescence quantum yield in a protein-free buffer among the compounds presented here. The quantum yields after protein addition were higher for the indolenine-based compounds shown here than for the benz[*e*]indole derivatives **2** and **3** (Φ_F = 25.0 and 36.3%, respectively [43]). Comparing the fluorescence intensities emitted after incubation of the dye with the highest concentration of protein tested, squaraine dye **5a** exhibited a 41-fold-higher peak fluorescence intensity in the presence of albumin. All others showed lower ratios (F/F_0 = 12–31), indicating a weaker interaction. The introduction of the dipicolylamino group markedly weakened its ability to interact *in vitro* with HSA. With an intermediate F/F_0 ratio, the diethanolamino-bearing benz[*e*]indole dye **11b** was shown to be the most sensitive (S = 5.5 × 10^5 nM), as well as the one with the lowest detection limit (DL = 168 nM), standing out as a potential means of detecting albumin in samples with very low levels of this protein. Given its low detection limit, squaraine **11b**'s limit of quantification was also low (QL < 1.2 μM), desirable features for its potential application in protein quantification. Squaraine dye **5a** exhibited a moderate detection limit (DL = 314 nM) and the highest quantification limit among the prepared dyes (QL = 1047 nM).

Compared to other dyes of the same family reported in the literature [61–63], those reported here generally showed slightly higher detection limits, but limits of quantification of the same order of magnitude or significantly higher (such as in the case of squaraine **5a**). Based on the results obtained for compounds **2** and **3** [43] and those reported here, it can be concluded that the functionalization with amines induces, in general, a very marked reduction in both determined limits. The introduction of the diethanolamino group vaguely improved the method's sensitivity, showing values two to five times higher than the indolenine zwitterionic dye **5a**. Comparisons with the benz[*e*]indole zwitterionic dye **1** were not possible, as it was not studied due to its high insolubility. At the same time, the functionalization with picolylamines seems to have reduced this parameter more evidently for the dyes with two pyridine moieties.

For the potential application of these dyes as fluorescent probes for the detection of albumins in human plasma samples, selectivity is an essential factor, and the interaction of the evaluated dyes with γ-globulins was compared. Squaraine dye **12a** showed the most remarkable difference between the intensity emitted in the presence of albumin and γ-globulins, showing a fluorescence intensity about fifteen times lower when incubated with globulins. The difference in fluorescence intensity emitted by squaraine **11b** in the presence of albumin and globulins was relatively small compared to the other compounds, showing poor selectivity. The applicability of the remaining molecules as albumin fluorescent probes is not questioned, showing fluorescence intensities five to ten times higher for HSA.

Molecular docking of the various dyes at Sudlow site I showed that the most predominant interactions are of a hydrophobic nature, similar to warfarin. Squaraines **11a**,**b** also showed interactions by hydrogen bonds, mainly involving the hydroxyl groups of the

diethanolamino group. Electrostatic interactions were also observed for dyes **5a**, **12a,** and **13a**. Although the squaraines exhibited an affinity for this receptor higher than warfarin, dyes **5a**, **11b**, and **13a** exhibited a negative charge repulsion due to their positive charge in the indole moieties. These unfavorable interactions are explained by the positively charged entrance of Sudlow site I, making this active site more appropriate for anionic ligands [58,60]. For Sudlow site II, all squaraine dyes showed considerably lower BE values than for site I, thus displaying less affinity for this site on the protein. Similar to site I, hydrophobic interactions were the most predominant, and classic hydrogen bond interactions were also observed for diethanolamino-loaded squaraines **11a**,**b,** and non-classical interactions for the benz[*e*]indole derivative **11b**. In general, for this site, squaraines **11b** and **13a** showed the best affinity *in silico* (BE = −10.21 and −9.41 Kcal/mol, respectively), while the remaining ones showed equivalent negative energies. Considering the protein as a whole, all evaluated squaraines displayed similar BE values, except for dye **11a**, which showed a lower interaction with human serum protein. Thus, the *in silico* studies, despite not allowing for differentiation of the interaction as accentuated as those observed in the fluorescence studies, allowed us to understand that Sudlow site I is the preferred active site for the interaction of all dyes with the HSA protein, since that it was for this that distinctly higher binding energies were calculated.

In the near future, our research group's objective is to carry out more in-depth selectivity studies in which other proteins, such as fibrinogen and hemoglobin, and other molecules such as amino acids, vitamins, hormones, and ions recurrently found in biological samples will be subjected to *in silico* and *in vitro* interaction studies. Furthermore, having verified a good selectivity index, we intend to compare the method using the potential fluorescent probe with traditionally used procedures to prove its reliability and validity.

5. Conclusions

We report an *in vitro* and computational study to verify the potential application of squaraine dyes derived from benz[*e*]indole and indolenine as fluorescent probes for detecting HSA proteins. All dyes showed a structure–relationship influence on the kinetic interaction with serum albumin, resulting in a significant increase in fluorescence intensity. After adding the squaraine solution to the HSA solution, the dye molecules interact with the protein primarily through hydrophobic interactions. Depending on the dye structure and limits of detection, the quantification and sensitivity diverge considerably, with indolenine-based zwitterionic squaraine dye showing properties closer to those desirable for a fluorescent probe. Functionalization with amines has reduced the detection and quantitation limits of squaraine dyes while maintaining worthy sensitivity. *In silico* studies show these compounds may bind to Sudlow site I and site II of HSA, with a preference for site I. When incubated with γ-globulins, the dyes emitted considerably lower fluorescence intensities than in the presence of HSA, suggesting good to excellent selectivity. Other selectivity studies are the next step to reiterate the interest in these compounds from the perspective of application in biological samples.

Supplementary Materials: The following supporting information can be downloaded at: https://www.mdpi.com/article/10.3390/chemosensors10080314/s1, Figure S1: ^{1}H NMR spectrum of squaraine dye **11a** (600 MHz, DMSO-d_6, ppm); Figure S2: ^{1}H NMR spectrum of squaraine dye **11a** (600 MHz, DMSO-d_6+D_2O ppm); Figure S3: ^{13}C NMR spectrum of squaraine dye **11a** (150.90 MHz, DMSO-d_6, ppm); Figure S4: ^{1}H NMR spectrum of squaraine dye **11b** (600 MHz, DMSO-d_6, ppm); Figure S5: ^{1}H NMR spectrum of squaraine dye **11b** (600 MHz, DMSO-d_6 + D_2O, ppm); Figure S6: ^{13}C NMR spectrum of squaraine dye **11b** (150.0 MHz, DMSO-d_6, ppm); Figure S7: ^{1}H NMR spectrum of squaraine dye **12a** (600 MHz, $CDCl_3$, ppm); Figure S8: ^{1}H NMR spectrum of squaraine dye **12a** (600 MHz, $CDCl_3$+D_2O, ppm); Figure S9: ^{13}C NMR spectrum of squaraine dye **12a** (150.0 MHz, $CDCl_3$, ppm); Figure S10: ^{1}H NMR spectrum of squaraine dye **13a** (400 MHz, DMSO-d_6, ppm); Figure S11: ^{13}C NMR spectrum of squaraine dye **13a** (150.0 MHz, DMSO-d_6, ppm); Figure S12: Visible absorption (Abs) and emission (Em) spectra of squaraine dyes **5a**, **11a**,**b**, **12a**, and **13a** obtained in dimethylformamide (DMF), dimethyl sulfoxide (DMSO) and chloroform (CFM). Absorbance and

fluorescence intensity were normalized to 1.0 for more straightforward analysis and are presented as arbitrary units (a.u.); Figure S13: Fluorescence spectra of squaraine dyes **5a**, **11a**,**b**, **12a**, and **13a** in phosphate buffer pH 7.4 at a concentration of 2.0 μM in the presence and absence of human γ-globulin and serum albumin proteins and at a concentration of 3.0 μM. Spectra were obtained at the incubation time with the highest albumin–dye interaction, and fluorescence intensity is presented as arbitrary units (a.u.); Table S1: Estimated free binding energy and interactions list of warfarin and squaraine dyes **5a**, **11a**,**b**, **12a**, and **13a** in Sudlow site I of human serum albumin; Table S2: Estimated free binding energy and interactions list of ibuprofen and squaraine dyes **5a**, **11a**,**b**, **12a**, and **13a** in Sudlow site II of human serum albumin; Table S3: Estimated free binding energy and interactions of squaraine dyes **5a**, **11a**,**b**, **12a**, and **13a** in human serum albumin; Figure S14: Binding modes and interactions of squaraine dyes **5a**, **11a**,**b**, **12a**, and **13a** with amino acid residues of human serum albumin protein.

Author Contributions: Conceptualization, M.A.S., E.L., O.F. and L.V.R.; Investigation, M.A.S., E.L., O.F., R.E.B., P.A. and L.V.R.; data curation, M.A.S., E.L. and O.F.; writing—original draft preparation, E.L. and O.F.; writing—review and editing, R.E.B., P.A. and L.V.R.; supervision, L.V.R. All authors have read and agreed to the published version of the manuscript.

Funding: The authors are thankful to the Portuguese Foundation for Science and Technology (FCT) and European Regional Development Fund (FEDER) for their financial support to the research centers CQVR (UID/QUI/UI0616/2019) and CICS-UBI (UIDB/00709/2020 and UIDP/00709/2020). The NMR spectrometers are part of the National NMR Network (PTNMR) and are partially supported by Infrastructure Project 022161 (co-financed by FEDER through COMPETE 2020, POCI and PORL and FCT through PIDDAC). Eurico Lima is also grateful to FCT for the PhD grant SFRH/BD/147645/2019.

Institutional Review Board Statement: Not applicable.

Informed Consent Statement: Not applicable.

Data Availability Statement: The data is available on the request from corresponding author.

Acknowledgments: Graphical abstract was created using Biorender.com (accessed on 15 June 2022).

Conflicts of Interest: The authors declare no conflict of interest. The funders had no role in the design of the study; in the collection, analyses, or interpretation of data; in the writing of the manuscript, or in the decision to publish the results.

References

1. Volkova, K.D.; Kovalska, V.B.; Losytskyy, M.Y.; Bento, A.; Reis, L.V.; Santos, P.F.; Almeida, P.; Yarmoluk, S.M. Studies of Benzothiazole and Benzoselenazole Squaraines as Fluorescent Probes for Albumins Detection. *J. Fluoresc.* **2008**, *18*, 877–882. [CrossRef] [PubMed]
2. Barbero, N.; Butnarasu, C.; Visentin, S.; Barolo, C. Squaraine Dyes: Interaction with Bovine Serum Albumin to Investigate Supramolecular Adducts with Aggregation-Induced Emission (AIE) Properties. *Chem. Asian J.* **2019**, *14*, 896–903. [CrossRef] [PubMed]
3. Zhang, Y.-Z.; Yang, Q.-F.; Du, H.-Y.; Tang, Y.-L.; Xu, G.-Z.; Yan, W.-P. Spectroscopic Investigation on the Interaction of a Cyanine Dye with Serum Albumins. *Chin. J. Chem.* **2008**, *26*, 397–401. [CrossRef]
4. Jahanban-Esfahlan, A.; Panahi-Azar, V. Interaction of Glutathione with Bovine Serum Albumin: Spectroscopy and Molecular Docking. *Food Chem.* **2016**, *202*, 426–431. [CrossRef] [PubMed]
5. Jurek, K.; Kabatc, J.; Kostrzewska, K. Fluorescent Amino-substituted Squaraine Probes for Bovine Serum Albumin. *Coloration Technol.* **2017**, *133*, 170–177. [CrossRef]
6. Luo, Z.; Liu, B.; Zhu, K.; Huang, Y.; Pan, C.; Wang, B.; Wang, L. An Environment-Sensitive Fluorescent Probe for Quantification of Human Serum Albumin: Design, Sensing Mechanism, and Its Application in Clinical Diagnosis of Hypoalbuminemia. *Dye. Pigm.* **2018**, *152*, 60–66. [CrossRef]
7. Hou, X.; Tong, X.; Dong, W.; Dong, C.; Shuang, S. Synchronous Fluorescence Determination of Human Serum Albumin with Methyl Blue as a Fluorescence Probe. *Spectrochim. Acta A Mol. Biomol. Spectrosc.* **2007**, *66*, 552–556. [CrossRef]
8. Levitt, D.; Levitt, M. Human Serum Albumin Homeostasis: A New Look at the Roles of Synthesis, Catabolism, Renal and Gastrointestinal Excretion, and the Clinical Value of Serum Albumin Measurements. *Int. J. Gen. Med.* **2016**, *9*, 229–255. [CrossRef]
9. Volkova, K.D.; Kovalska, V.B.; Losytskyy, M.Y.; Reis, L.V.; Santos, P.F.; Almeida, P.; Lynch, D.E.; Yarmoluk, S.M. Aza-Substituted Squaraines for the Fluorescent Detection of Albumins. *Dye. Pigm.* **2011**, *90*, 41–47. [CrossRef]
10. Li, P.; Wang, Y.; Zhang, S.; Xu, L.; Wang, G.; Cui, J. An Ultrasensitive Rapid-Response Fluorescent Probe for Highly Selective Detection of HSA. *Tetrahedron Lett.* **2018**, *59*, 1390–1393. [CrossRef]

11. Xiong, J.; Cao, X.; Yang, S.; Mo, Z.; Wang, W.; Zeng, W. Fluorescent Probes for Detection of Protein: From Bench to Bed. *Protein Pept. Lett.* **2018**, *25*, 548–559. [CrossRef] [PubMed]
12. Wang, N.; Xin, C.; Li, Z.; Zhang, G.; Bai, L.; Gong, Q.; Xu, C.; Han, X.; Yu, C.; Li, L.; et al. A Reversible Fluorescent Probe for Directly Monitoring Protein-Small Molecules Interaction Utilizing Vibration-Induced Emission. *Dye. Pigm.* **2019**, *163*, 425–432. [CrossRef]
13. Sargazi, S.; Fatima, I.; Hassan Kiani, M.; Mohammadzadeh, V.; Arshad, R.; Bilal, M.; Rahdar, A.; Díez-Pascual, A.M.; Behzadmehr, R. Fluorescent-Based Nanosensors for Selective Detection of a Wide Range of Biological Macromolecules: A Comprehensive Review. *Int. J. Biol. Macromol.* **2022**, *206*, 115–147. [CrossRef]
14. Camarca, A.; Varriale, A.; Capo, A.; Pennacchio, A.; Calabrese, A.; Giannattasio, C.; Murillo Almuzara, C.; D'Auria, S.; Staiano, M. Emergent Biosensing Technologies Based on Fluorescence Spectroscopy and Surface Plasmon Resonance. *Sensors* **2021**, *21*, 906. [CrossRef] [PubMed]
15. Li, H.; Yao, Q.; Fan, J.; Du, J.; Wang, J.; Peng, X. An NIR Fluorescent Probe of Uric HSA for Renal Diseases Warning. *Dye. Pigm.* **2016**, *133*, 79–85. [CrossRef]
16. Kim, Y.; Shin, E.; Jung, W.; Kim, M.K.; Chong, Y. A Near-Infrared Turn-on Fluorescent Sensor for Sensitive and Specific Detection of Albumin from Urine Samples. *Sensors* **2020**, *20*, 1232. [CrossRef]
17. Aristova, D.; Volynets, G.; Chernii, S.; Losytskyy, M.; Balanda, A.; Slominskii, Y.; Mokhir, A.; Yarmoluk, S.; Kovalska, V. Far-Red Pentamethine Cyanine Dyes as Fluorescent Probes for the Detection of Serum Albumins. *R. Soc. Open Sci.* **2020**, *7*, 200453. [CrossRef]
18. Xu, Y.; Li, B.; Li, W.; Zhao, J.; Sun, S.; Pang, Y. "ICT-Not-Quenching" near Infrared Ratiometric Fluorescent Detection of Picric Acid in Aqueous Media. *Chem. Commun.* **2013**, *49*, 4764–4766. [CrossRef]
19. Ananda Rao, B.; Kim, H.; Son, Y.-A. Synthesis of Near-Infrared Absorbing Pyrylium-Squaraine Dye for Selective Detection of Hg^{2+}. *Sens. Actuators B Chem.* **2013**, *188*, 847–856. [CrossRef]
20. Hu, L.; Zhang, Y.; Nie, L.; Xie, C.; Yan, Z. Colorimetric Detection of Trace Hg^{2+} with Near-Infrared Absorbing Squaraine Functionalized by Dibenzo-18-Crown-6 and Its Mechanism. *Spectrochim. Acta A Mol. Biomol. Spectrosc.* **2013**, *104*, 87–91. [CrossRef]
21. Wang, W.; Fu, A.; Lan, J.; Gao, G.; You, J.; Chen, L. Rational Design of Fluorescent Bioimaging Probes by Controlling the Aggregation Behavior of Squaraines: A Special Effect of Ionic Liquid Pendants. *Chem. Eur. J.* **2010**, *16*, 5129–5137. [CrossRef] [PubMed]
22. Wallace, K.J.; Gray, M.; Zhong, Z.; Lynch, V.M.; Anslyn, E.V. An Artificial Siderophore for the Detection of Iron(III). *Dalton Trans.* **2005**, *14*, 2436–2441. [CrossRef] [PubMed]
23. Wang, W.; Fu, A.; You, J.; Gao, G.; Lan, J.; Chen, L. Squaraine-Based Colorimetric and Fluorescent Sensors for Cu^{2+}-Specific Detection and Fluorescence Imaging in Living Cells. *Tetrahedron* **2010**, *66*, 3695–3701. [CrossRef]
24. Sanna, E.; Martínez, L.; Rotger, C.; Blasco, S.; González, J.; García-España, E.; Costa, A. Squaramide-Based Reagent for Selective Chromogenic Sensing of Cu(II) through a Zwitterion Radical. *Org. Lett.* **2010**, *12*, 3840–3843. [CrossRef]
25. Huang, Y.; Lin, Q.; Wu, J.; Fu, N. Design and Synthesis of a Squaraine Based Near-Infrared Fluorescent Probe for the Ratiometric Detection of Zn^{2+} Ions. *Dye. Pigm.* **2013**, *99*, 699–704. [CrossRef]
26. Jiang, J.-Q.; Sun, C.-L.; Shi, Z.-F.; Xu, Z.-G.; Zhang, H.-L. A Ppb Level Turn-on Fluorescence Chemosensor for the Detection of Zn^{2+}. *Sens. Actuators B Chem.* **2015**, *220*, 659–664. [CrossRef]
27. Basheer, M.C.; Alex, S.; George Thomas, K.; Suresh, C.H.; Das, S. A Squaraine-Based Chemosensor for Hg^{2+} and Pb^{2+}. *Tetrahedron* **2006**, *62*, 605–610. [CrossRef]
28. Hsueh, S.-Y.; Lai, C.-C.; Liu, Y.-H.; Wang, Y.; Peng, S.-M.; Chiu, S.-H. Protecting a Squaraine Near-IR Dye through Its Incorporation in a Slippage-Derived [2]Rotaxane. *Org. Lett.* **2007**, *9*, 4523–4526. [CrossRef]
29. Fan, X.; Zhang, D.; Li, H.; Sun, S.; Xu, Y. A BSA-Squaraine Hybrid System for Selectively Detecting Ag^{+} in Absolute PBS and Sequential Construction of Logic Functions. *Sens. Actuators B Chem.* **2017**, *245*, 290–296. [CrossRef]
30. Arunkumar, E.; Ajayaghosh, A.; Daub, J. Selective Calcium Ion Sensing with a Bichromophoric Squaraine Foldamer. *J. Am. Chem. Soc.* **2005**, *127*, 3156–3164. [CrossRef]
31. Gassensmith, J.J.; Matthys, S.; Lee, J.-J.; Wojcik, A.; Kamat, P.V.; Smith, B.D. Squaraine Rotaxane as a Reversible Optical Chloride Sensor. *Chem. Eur. J.* **2010**, *16*, 2916–2921. [CrossRef] [PubMed]
32. Elmes, R.B.P.; Turner, P.; Jolliffe, K.A. Colorimetric and Luminescent Sensors for Chloride: Hydrogen Bonding vs Deprotonation. *Org. Lett.* **2013**, *15*, 5638–5641. [CrossRef] [PubMed]
33. Zhang, Y.; Jiang, H.; Wang, X. Cytidine-Stabilized Gold Nanocluster as a Fluorescence Turn-on and Turn-off Probe for Dual Functional Detection of Ag^{+} and Hg^{2+}. *Anal. Chim. Acta* **2015**, *870*, 1–7. [CrossRef] [PubMed]
34. Li, J.; Ji, C.; Yang, W.; Yin, M. PH Switchable and Fluorescent Ratiometric Squarylium Indocyanine Dyes as Extremely Alkaline Solution Sensors. *Analyst* **2013**, *138*, 7289–7293. [CrossRef] [PubMed]
35. Hovor, I.V.; Kolosova, O.S.; Sanin, E.V.; Obukhova, O.M.; Tatarets, A.L.; Terpetschnig, E.A.; Patsenker, L.D. Water-Soluble Norsquaraine Dyes for Protein Labeling and PH-Sensing Applications. *Dye. Pigm.* **2019**, *170*, 107567. [CrossRef]
36. Butnarasu, C.; Barbero, N.; Barolo, C.; Visentin, S. Squaraine Dyes as Fluorescent Turn-on Sensors for the Detection of Porcine Gastric Mucin: A Spectroscopic and Kinetic Study. *J. Photochem. Photobiol. B Biol.* **2020**, *205*, 111838. [CrossRef]

37. Butnarasu, C.; Barbero, N.; Barolo, C.; Visentin, S. Interaction of Squaraine Dyes with Proteins: Looking for More Efficient Fluorescent Turn-on Probes. *Dye. Pigm.* **2021**, *184*, 108873. [CrossRef]
38. Xu, Y.; Li, B.; Han, P.; Sun, S.; Pang, Y. Near-Infrared Fluorescent Detection of Glutathione via Reaction-Promoted Assembly of Squaraine-Analyte Adducts. *Analyst* **2013**, *138*, 1004–1007. [CrossRef]
39. Zheng, Z.; Huyan, Y.; Li, H.; Sun, S.; Xu, Y. A Lysosome-Targetable near Infrared Fluorescent Probe for Glutathione Sensing and Live-Cell Imaging. *Sens. Actuators B Chem.* **2019**, *301*, 127065. [CrossRef]
40. Liu, T.; Huo, F.; Yin, C.; Li, J.; Niu, L. A Highly Selective Fluorescence Sensor for Cysteine/Homocysteine and Its Application in Bioimaging. *RSC Adv.* **2015**, *5*, 28713–28716. [CrossRef]
41. Shahrokhian, S. Lead Phthalocyanine as a Selective Carrier for Preparation of a Cysteine-Selective Electrode. *Anal. Chem.* **2001**, *73*, 5972–5978. [CrossRef] [PubMed]
42. Refsum, H.; Smith, A.D.; Ueland, P.M.; Nexo, E.; Clarke, R.; McPartlin, J.; Johnston, C.; Engbaek, F.; Schneede, J.; McPartlin, C.; et al. Facts and Recommendations about Total Homocysteine Determinations: An Expert Opinion. *Clin. Chem.* **2004**, *50*, 3–32. [CrossRef] [PubMed]
43. Lima, E.; Barroso, A.G.; Sousa, M.A.; Ferreira, O.; Boto, R.E.; Fernandes, J.R.; Almeida, P.; Silvestre, S.M.; Santos, A.O.; Reis, L.V. Picolylamine-Functionalized Benz[*e*]Indole Squaraine Dyes: Synthetic Approach, Characterization and in Vitro Efficacy as Potential Anticancer Phototherapeutic Agents. *Eur. J. Med. Chem.* **2022**, *229*, 114071. [CrossRef]
44. Ogunsipe, A.; Maree, D.; Nyokong, T. Solvent Effects on the Photochemical and Fluorescence Properties of Zinc Phthalocyanine Derivatives. *J. Mol. Struct.* **2003**, *650*, 131–140. [CrossRef]
45. Lister, A.S. 7 Validation of HPLC Methods in Pharmaceutical Analysis. In *Separation Science and Technology*; Elsevier: Amsterdam, The Netherlands, 2005; Volume 6, pp. 191–217. ISBN 978-0-12-088547-3.
46. Pires, D.E.V.; Blundell, T.L.; Ascher, D.B. PkCSM: Predicting Small-Molecule Pharmacokinetic and Toxicity Properties Using Graph-Based Signatures. *J. Med. Chem.* **2015**, *58*, 4066–4072. [CrossRef]
47. Lima, E.; Ferreira, O.; Gomes, V.S.D.; Santos, A.O.; Boto, R.E.; Fernandes, J.R.; Almeida, P.; Silvestre, S.M.; Reis, L.V. Synthesis and in Vitro Evaluation of the Antitumoral Phototherapeutic Potential of Squaraine Cyanine Dyes Derived from Indolenine. *Dye. Pigm.* **2019**, *167*, 98–108. [CrossRef]
48. Lima, E.; Ferreira, O.; Silva, J.F.; Santos, A.O.; Boto, R.E.; Fernandes, J.R.; Almeida, P.; Silvestre, S.M.; Reis, L.V. Photodynamic Activity of Indolenine-Based Aminosquaraine Cyanine Dyes: Synthesis and in Vitro Photobiological Evaluation. *Dye. Pigm.* **2020**, *174*, 108024. [CrossRef]
49. Lima, E.; Boto, R.E.; Ferreira, D.; Fernandes, J.R.; Almeida, P.; Ferreira, L.F.V.; Souto, E.B.; Silva, A.M.; Reis, L.V. Quinoline- and Benzoselenazole-Derived Unsymmetrical Squaraine Cyanine Dyes: Design, Synthesis, Photophysicochemical Features and Light-Triggerable Antiproliferative Effects against Breast Cancer Cell Lines. *Materials* **2020**, *13*, 2646. [CrossRef]
50. Reis, L.; Serrano, J.; Almeida, P.; Santos, P. The Synthesis and Characterization of Novel, Aza-Substituted Squarylium Cyanine Dyes. *Dye. Pigm.* **2009**, *81*, 197–202. [CrossRef]
51. Reis, L.V.; Serrano, J.P.; Almeida, P.; Santos, P.F. New Synthetic Approach to Aminosquarylium Cyanine Dyes. *Synlett* **2002**, *10*, 1617–1620. [CrossRef]
52. Oushiki, D.; Kojima, H.; Takahashi, Y.; Komatsu, T.; Terai, T.; Hanaoka, K.; Nishikawa, M.; Takakura, Y.; Nagano, T. Near-Infrared Fluorescence Probes for Enzymes Based on Binding Affinity Modulation of Squarylium Dye Scaffold. *Anal. Chem.* **2012**, *84*, 4404–4410. [CrossRef] [PubMed]
53. Lakowicz, J.R. *Principles of Fluorescence Spectroscopy*, 3rd ed.; Springer: New York, NY, USA, 2006; ISBN 978-0-387-31278-1.
54. Zhang, Y.; Yue, X.; Kim, B.; Yao, S.; Bondar, M.V.; Belfield, K.D. Bovine Serum Albumin Nanoparticles with Fluorogenic Near-IR-Emitting Squaraine Dyes. *ACS Appl. Mater. Interfaces* **2013**, *5*, 8710–8717. [CrossRef] [PubMed]
55. McKerrow, A.J.; Buncel, E.; Kazmaier, P.M. Aggregation of Squaraine Dyes: Structure–Property Relationships and Solvent Effects. *Can. J. Chem.* **1995**, *73*, 1605–1615. [CrossRef]
56. Fernandes, T.C.D.; Lima, E.; Boto, R.E.; Ferreira, D.; Fernandes, J.R.; Almeida, P.; Ferreira, L.F.V.; Silva, A.M.; Reis, L.V. In Vitro Phototherapeutic Effects of Indolenine-Based Mono- and Dithiosquaraine Cyanine Dyes against Caco-2 and HepG2 Human Cancer Cell Lines. *Photodiagnosis Photodyn. Ther.* **2020**, *31*, 101844. [CrossRef]
57. Sugio, S.; Kashima, A.; Mochizuki, S.; Noda, M.; Kobayashi, K. Crystal Structure of Human Serum Albumin at 2.5 Å Resolution. *Protein Eng. Des. Sel.* **1999**, *12*, 439–446. [CrossRef] [PubMed]
58. Ghuman, J.; Zunszain, P.A.; Petitpas, I.; Bhattacharya, A.A.; Otagiri, M.; Curry, S. Structural Basis of the Drug-Binding Specificity of Human Serum Albumin. *J. Mol. Biol.* **2005**, *353*, 38–52. [CrossRef]
59. Wzorek, J.; Bednarek, R.; Watala, C.; Boncler, M. Efficacy of a Combined Antiplatelet Therapy Is Not Affected by a Simultaneous Binding of Cangrelor and PSB 0777 to Albumin. *Front. Pharmacol.* **2021**, *12*, 638257. [CrossRef]
60. Al-Harthi, S.; Lachowicz, J.I.; Nowakowski, M.E.; Jaremko, M.; Jaremko, Ł. Towards the Functional High-Resolution Coordination Chemistry of Blood Plasma Human Serum Albumin. *J. Inorg. Biochem.* **2019**, *198*, 110716. [CrossRef]
61. Gomes, V.S.D.; Ferreira, J.C.C.; Boto, R.E.F.; Almeida, P.; Fernandes, J.R.; Sousa, M.J.; Gonçalves, M.S.T.; Reis, L.V. Squaraine Dyes Derived from Indolenine and Benzo[*e*]Indole as Potential Fluorescent Probes for HSA Detection and Antifungal Agents. *Photochem. Photobiol.* **2022**, php.13624. [CrossRef]

62. Gomes, V.S.D.; Boto, R.E.F.; Almeida, P.; Coutinho, P.J.G.; Pereira, M.R.; Gonçalves, M.S.T.; Reis, L.V. Squaraine Dyes as Serum Albumins Probes: Synthesis, Photophysical Experiments and Molecular Docking Studies. *Bioorg. Chem.* **2021**, *115*, 105221. [CrossRef]
63. Gomes, V.S.D.; Gonçalves, H.M.R.; Boto, R.E.F.; Almeida, P.; Reis, L.V. Barbiturate Squaraine Dyes as Fluorescent Probes for Serum Albumins Detection. *J. Photochem. Photobiol. A Chem.* **2020**, *400*, 112710. [CrossRef]